Speckle imaging in Merate. The PISCO project: results and prospects

R. W. Argyle[∗], M. Scardia[†], J.-L. Prieur[∗∗] and L. Pansecchi[‡]

[∗]*Institute of Astronomy, Madingley Road, Cambridge, CB3 0HA, UK*
[†]*I.N.A.F. - Osservatorio Astronomico di Brera, Via E. Bianchi 46, 23807, Merate, Italy*
[∗∗]*Laboratoire d'Astrophysique de Toulouse-Tarbes, Université de Toulouse, CNRS, 14 avenue E. Belin, 31400 Toulouse, France*
[‡]*Osservatorio Astronomico di Brera, Via E. Bianchi 46, 23807, Merate, Italy*

Abstract. The PISCO project being carried out at I.N.A.F. - Osservatorio Astronomico di Brera (Merate, Italy) since 2003 is described. The aims of the project are outlined and results of work carried out so far are given. Prospects of extending and improving the scientific reach of the project using more efficient detectors on bigger telescopes are discussed.

Keywords: binaries: close, visual – astrometry – techniques: interferometric – stars: individual (gamma Virginis, ADS 8630)
PACS: To be determined

INTRODUCTION

The PISCO instrument

PISCO stands for the Pupil Interferometer Speckle Camera and Coronagraph. It is a multi-functional instrument which has been used to carry out speckle imaging of visual binary stars since 2003. The instrument was built at the Observatoire de Midi-Pyrenees by J.-L. Prieur and colleagues ([6]) and was first used at the 2-metre Telescope Bernard Lyot at the Observatoire du Pic du Midi in 1993 but by 1999 the time allocation panels were no longer allocating telescope time. In October 2003 the instrument was transferred to Merate, some 30 km north-east of Milan where it was fitted to the 1.02-metre Zeiss reflector (Fig. 1) and has been in regular use ever since producing to date more than 2,000 high quality measurements ([9], [10], [12], [14], [7], [16], [17], [18], [8], herein: Papers I to IX), from which we derived many new orbits (see e.g. [15]).

PISCO was designed to be a multi-purpose instrument offering full remote control of all its operating modes (see Fig. 2). It offers a wide range of possibilities with fast switching between modes (less than one minute) allowing optimal use of the seeing conditions. It is fully computer controlled and all its functions can be selected by a simple mouse click (see Fig. 3).

Its main features are listed here:

- **Full pupil imaging**: speckle imaging;
- **Masked pupil imaging**: aperture synthesis;
- **Coronagraphy**: imaging with a pupil mask;

 

FIGURE 1. PISCO (right) fitted to the 1.02-metre Zeiss reflector in Merate

- **Spectroscopy**: high angular resolution along the slit;
- **Pupil plane imaging**: SCIDAR (SCintillation Detection And Ranging) or Shack-Hartman with an array of micro-lenses.

In this paper the full pupil imaging mode is described in detail and its use in the observation of the relative positions of the components of close visual binary star systems with speckle interferometric techniques.

Speckle interferometry

Large telescopes produce images of stars which are spread out into a time-averaged structure called the seeing disk under the influence of atmospheric turbulence. The seeing disk may be typically 1 arc second in diameter but very short exposures, typically 10 milliseconds, taken at high magnification, reveal structures called speckles which represent diffraction limited information. If a star is a close double then pairs of speckles separated by the angular separation, ρ of the double star can be seen in each short exposure. The speckles could be measured from these frames to yield separation and position angle (θ), but a more elegant way to obtain the data is to use Fourier techniques as proposed by Antoine Labeyrie in the 1970's ([4]).

The Fourier transform assesses the essence of the frequency of spatial speckle separation, and the power spectrum shows a set of fringes. By transforming again this image the autocorrelation is formed and this appears as a central spot with the equidistant satellite

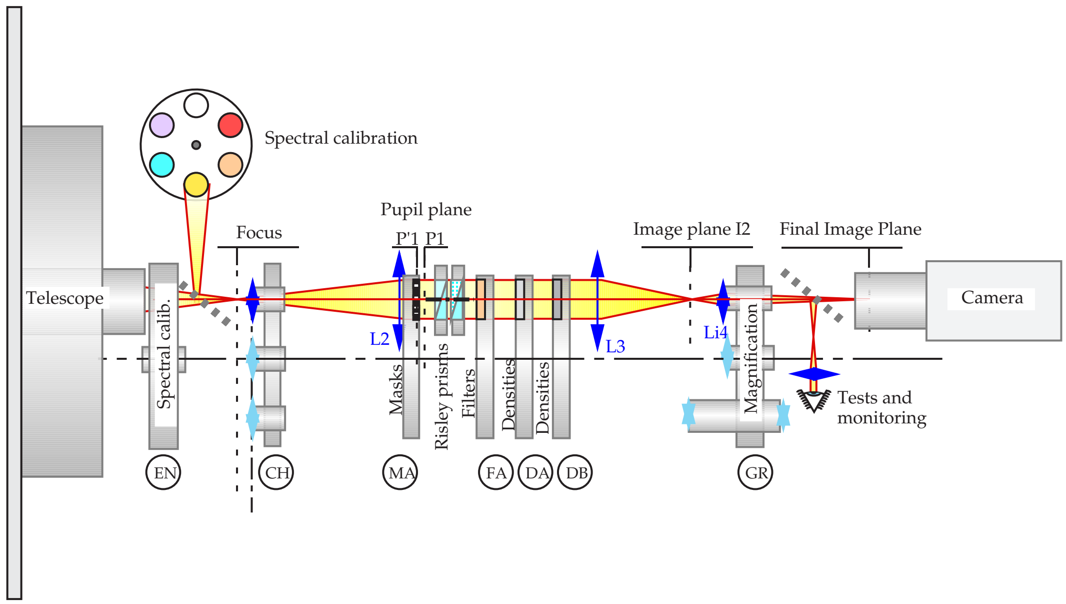

FIGURE 2. The optical layout of PISCO

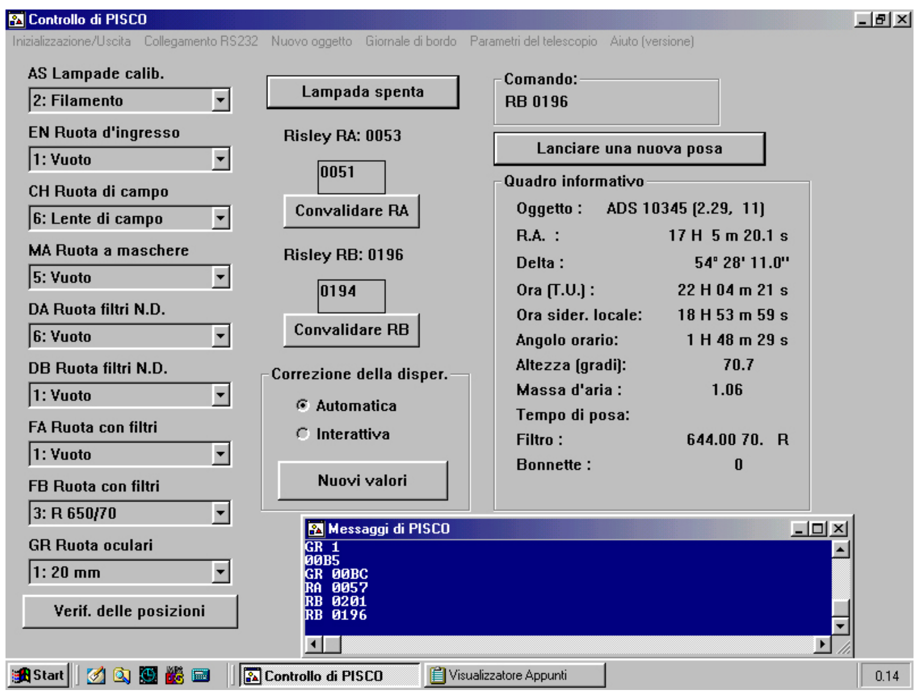

FIGURE 3. PISCO control panel in Merate.

images in which the orientation and spacing of the satellite images are directly related to position angle and separation.

The main methods used for achieving high resolution imaging are presented in Fig. 4 . Our team uses both the conventional speckle technique ([4]), that leads to astrometric

$$I_0(\vec{x}) \longrightarrow \boxed{\begin{array}{c} \textit{Atmosphere} + \textit{Telescope} \\ \mathrm{PSF:}\ H(\vec{x},t) \end{array}} \longrightarrow I_i(\vec{x},t)$$

- Data processing of short exposures:
  - Image selection: lucky imaging
  - Spectral analysis: speckle interferometry
  - Multi-spectral analysis: bispectral imaging
- Real-time correction of the wavefront: adaptive optics

FIGURE 4. Methods for achieving high angular resolution imaging through the atmosphere.

measurements of binary stars down to the diffraction limit of the telescope and the bispectral imaging methods first proposed by Weigelt ([19]), that allow the restoration of high resolution images. The latter is more complex to implement and we only use it when it brings useful information about the object (e.g., for triple or quadruple star systems).

OBSERVATIONS AND MEASUREMENTS

Description of our catalogue of targets

The purpose of the long-term PISCO programme is to monitor the relative motion of all the visual binaries accessible with this instrument, fitted to the Zeiss telescope of the I.N.A.F. - Osservatorio Astronomico di Brera in Merate (Italy), for which new measurements are needed to improve orbits. The sample consists of visual binaries with the following characteristics, which are imposed by instrumental or atmospheric limitations.

(i) declination: north of $-5°$;
(ii) magnitude: brighter than 9.5 - 10.0 in V;
(iii) magnitude difference: less than 4;
(iv) minimum angular separation: $0''.13$ in R;
(v) maximum angular separation: smaller than $\sim 4''.5$.

Limitation (iv) is imposed by the diffraction limit of the Zeiss telescope of 1.02 metre aperture, whilst limitation (v) is chosen so that the binary systems fit inside the isoplanatic patch of the atmosphere, which is a theoretical necessary condition for speckle measurements.

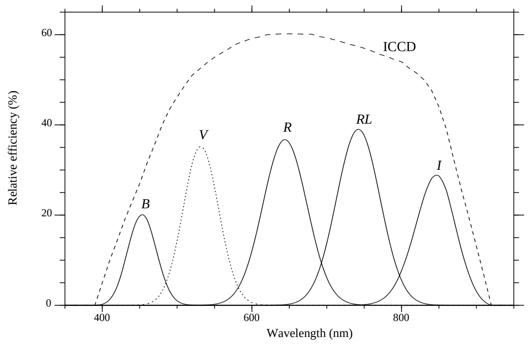

Name	Identification	λ_c (nm)	Δ_λ (nm)
B	ORIEL/57541	447	47
V	ORIEL/57581	530	57
R	ORIEL/57621	644	70
RL	ORIEL/57661	743	69
I	ORIEL/57701	855	74
W	ICCD alone	650	420

FIGURE 5. Characteristics of the filters available for use with PISCO.

Method of observation

The filters available in the PISCO wheels are presented in (Fig. 5). Some objects are even observed with no filter when they are too faint. This is indicated as *W* (for “white” light) in the name column of the table of Fig. 5. The corresponding bandpass and central wavelength correspond to that of the ICCD detector.

Usually, most of the observations are made in *R* through the eyepiece of 20 mm focal length, which gives a scale of 0.07517 arcsec per pixel. For particularly faint objects, we use this eyepiece and the *W* filter. In this case, however, the minimum separation stops at about 0".3, since in white light the autocorrelation peaks are less sharp.

The binaries with a separation smaller than 1".0 and a sufficient brightness (say, magnitude smaller than 8) are observed through the 10 mm eyepiece which gives a scale of 0.03202 arcsec per pixel.

In the case of binaries with components having a large difference of magnitude, and, likely, different spectral class, we have found it useful to observe through the *RL* (Deep Red) filter. This usually reduces the difference of brightness between the components, allowing to take advantage of the fact that at whose wavelengths the seeing is better, and, in conclusion, delivers sharper autocorrelation peaks.

The exposure time of the ICCD can be set from 4 ms up to 16 ms (milliseconds), which is the upper limit imposed by the technical characteristics of this detector. The optimum value depends on the brightness of the objects, on the seeing, and on the sky transparency. On average, it is of the order of 8-12 ms.

Each observation (or measure) consists in the acquisition of about 10,000-12,000 elementary frames, each taken with the above mentioned exposure time, with the possibility of selecting, in real time, only the best images as done, substantially, by ‘lucky’ imaging ([5]). The images, each 128 x 128 pixels in size, are recorded in real time at the rate of 50 images per second, so the total integration time lasts about 4-5 minutes.

Real-time processing of the incoming images is performed on a PC equipped with an Rio/Ellips analog/digital converter board. The specially-designed program *vcrb* retrieves data cubes from the memory of this board, and performs various calculations on those frames, after subtraction of bias and flat fielding. This program can also work with FITS data cubes of elementary frames, which allows the re-processing of the recorded

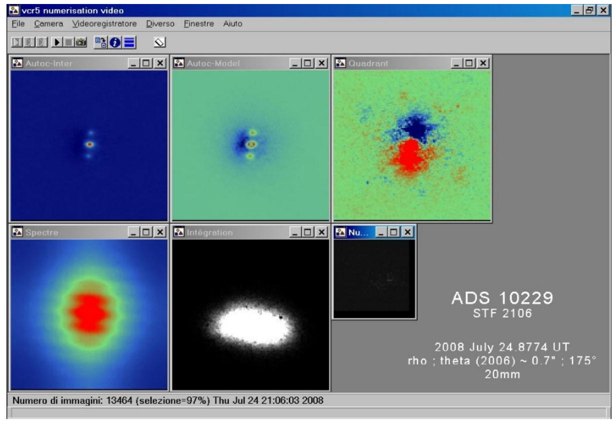

FIGURE 6. Example of real-time processing of PISCO observations with ADS 10229. From left to right and top to bottom: autocorrelation, autocorrelation minus background model, restricted triple-correlation, power spectrum, long integration, elementary frame.

data.

With the program `vcrb` during the exposure a total of six windows, continuously updating, are observed on the computer screen. We give an example of such display in Fig. 6. From left to right and top to bottom, the program displays:

- the mean autocorrelation, with two symmetric peaks in the case of resolved binaries (with most of the background removed, using Worden's method [20]),
- the same autocorrelation but with the subtraction of a model obtained from an unresolved (or single) star, which is useful in the case of very close binaries whose secondary peaks (autocorrelations) could be embedded in the central peak,
- the real-time, triple-correlation analysis ([1]) of the elementary frames allows to discriminate the quadrant of the companion, which usually presents a 180 degree ambiguity in the speckle interferometry.
- the mean power spectrum,
- the mean image ("long integration")
- the real time image

At the end of each observation, the result is saved on disk as files in FITS format: the long integration (*_l.fits), the mean power spectrum (*_m.fits), Worden's mean autocorrelation (*_a.fits), and the restricted mean triple-correlation (*_q.fits), that is used for quadrant determination.

There is also the possibility of also computing the mean bispectrum that is necessary for full image restoration ([19]). This is seldom used during the observations because it is time-consuming. The bispectrum can be computed *a posteriori* with the recorded elementary frames.

Since September 2009, the elementary frames, which, typically, occupy a memory of 250-300 MB, are also saved on a hard disc of high capacity (2TB) for possible future elaborations. Before this date, the elementary frames were recorded on SVHS tapes.

FIGURE 7. Grating mask mounted on the Zeiss telescope for scale absolute calibration, and some members of the PISCO team (from left to right: J.-L. Prieur, M. Scardia, R. Valtolina, L. Pansecchi).

Data reduction

The reduction of the recorded files is made on a second step, with interactive programs, during daytime. Currently two programs can be used for this purpose: the old `Xdisp1` in C that uses the X11 library and can be only used on UNIX/LINUX computers, and the new `Wdisp1` in C++, that uses the multi-platform graphic library `wxwidgets` and can be run both Linux and Windows environments. The derivation of the measures is identical in both programs. The only difference is that the new program `Wdisp1` has a more user-friendly interface.

The procedure starts by displaying the mean Worden's autocorrelation image which is in the form of a standard FITS file. It is then followed by:

1. A circle of variable diameter is interactively selected by the observer so that it comfortably encloses the secondary peak.
2. The background of the image is then automatically fitted outside this circle and then subtracted inside this circle. Two methods are available. In the "patch" method, a 2D polynomial is fitted within a circular annulus around this circle. In the "profile" method, a 1D polynomial is fitted to the profile computed in a region close to the peak.
3. After subtracting this background, the program computes the accurate position of the centroid of the secondary peak inside the selected circle. This is done in two different ways, by a barycentric calculation and by Gaussian profile fitting.

In the procedure we use, at least two different circles are interactively selected for each of the two secondary peaks, which thus lead to at least eight determinations of both position angle and separation. The program then computes the mean and standard deviation of the measurements and stores the result in a LateX-formatted file.

In the case of very close pairs, a 2D model can be fitted and subtracted from the observed autocorrelation (see Fig 8). This allows us to measure separations close to the diffraction limit and even slightly smaller than this value. In fact, the diffraction limit is not a rigid boundary and measurements of binaries can be obtained below this limit in

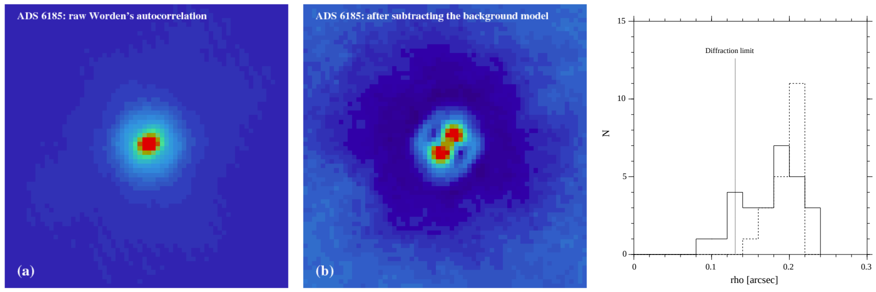

FIGURE 8. Processed autocorrelation (b) of the close binary ADS 6185 ($\rho = 0".085$), obtained by subtracting a model of the central background pattern from the auto-correlation (a). Right: distribution of the ρ measurements of 2004-2005 obtained with this procedure (solid line) compared to unprocessed ones (dashed line). The diffraction limit λ/D for the R filter and the 102-cm Zeiss telescope is indicated for comparison (Paper IV).

favourable conditions.

The angular scale of the images on the detector is determined using an objective grating (see Fig. 7), and the position angle is calibrated by measuring star trails produced when stopping the right-ascension motors. The formal error on our measures is $0^\circ.6$ and $0".01$.

Computation of visual binary orbits

Using Kepler's laws, the orbital parameters can lead to the determination of the total mass of a binary system. This is why it is so important to observe the apparent orbit of binary stars. This is achieved by measuring the relative position of the fainter component of the double star with respect to the brighter one (ρ and θ) with time.

Although speckle interferometry observations lead to measurements of much greater accuracy than was possible with visual observations, orbital analysis is still reliant on historical measures. This is due to the long length of orbital periods involved - typically tens to thousands of years.

Once the apparent orbit is defined, the true orbit can be determined and from the size of the semi-major axis, a, and period of revolution, P. The total stellar mass in the binary in terms of the sun's mass can be determined if the parallax, π is known. Because the masses (and therefore the observational errors in these masses) depend on higher powers of a, π and P it is necessary to determine these latter quantities as accurately as possible.

For orbital couples, we compute the residuals between our measurements and the ephemerides. When those residuals are large and when a significant number of measurements has been made since the last orbit computation, we compute a new revised orbit. We only revise orbits when it is really justified. For the binaries for which no orbit is know yet, when the number of measurements becomes sufficient, we also compute a new orbit.

For computing those orbits, we start by adding our observations to the other available observations contained in the data base maintained by the United States Naval Observatory. Our next step is to compute the preliminary orbital elements with the analytical method of Kowalsky ([3]). We then use them as initial values for the Hellerich's least-squares method ([2]). When convergence is achieved, Hellerich's method leads to an improvement of the orbital elements with an estimation of their errors.

MAIN RESULTS

Astrometric measurements

Since 1st January 2004, more than 2,000 high quality measurements of visual binaries have been made at Merate with typical accuracies of around $0''.01$ and $0^\circ.6$, with a limiting separation close to the diffraction limit of the telescope. The results have been discussed in twelve papers and have also resulted in 32 new or improved orbits being calculated (see next section).

The distribution of the angular separations is displayed in Fig. 9a and shows a maximum for $\rho \approx 0''.7$, with a full range between $0''.1$ and $4''.6$. Some measurements were even obtained below the diffraction limit $\rho_d = \lambda/D \approx 0''.13$ with the R filter (i.e. $\lambda = 650$ nm) and the Zeiss telescope whose aperture is $D = 1.02$ m. The smallest separation was measured for WRH 28 with $\rho = 0''.066 \pm 0.012$ (Paper IV).

Using the Hipparcos parallaxes, we were able to construct the HR diagram of those binaries that is displayed in Fig. 9b. We only plotted the objects for which the relative uncertainty on the parallax was smaller than 20%. It can be seen that a large part of the HR diagram is covered by our sample. In the future we would like to acquire a more sensitive detector in order to observe fainter (and cooler) main sequence stars.

The distribution of the apparent magnitudes m_V of the binaries measured between 2004 and 2008 is presented in Fig. 10a and the difference of magnitudes Δm_V between the two components in Fig. 10b. The telescope aperture and detector sensitivity lead to a limiting magnitude of about $m_V = 9.5$. A careful handling of the image processing enabled us to measure a few couples with $\Delta m_V > 3$ (Fig. 10c). The distribution of the errors on ρ (angular separation) shown in Fig. 10c shows that typical accuracy is around $0''.01$. For the position angle, it is about $0^\circ.6$.

Restored images with bispectral methods

We also restored images using bispectral techniques, that we specially adapted to our detector (intensified CCD). The main problem we faced concerned the correction of the bispectrum (see e.g. Fig. 11). for the bias introduced by the photon noise. We managed to implement our method in a fully non-supervised mode, so that restored images can be obtained automatically and displayed during the observations. Some examples of restored images from PISCO observations made at the Pic du Midi and in Merate are shown in Fig 12.

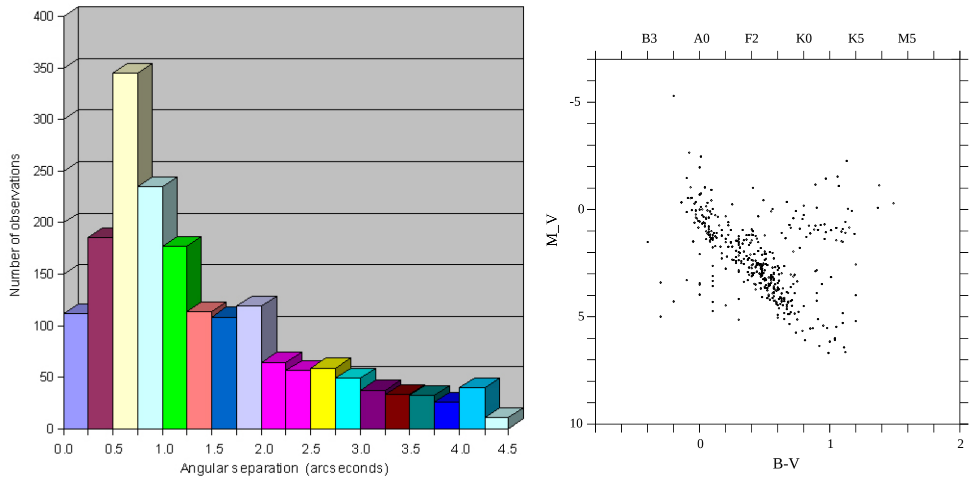

FIGURE 9. Distribution of angular separations of the binaries measured with PISCO in Merate in 2004-2008 (left) and corresponding HR diagram for the objects for which Hipparcos parallaxes were obtained with a relative error smaller than 20% (810 objects).

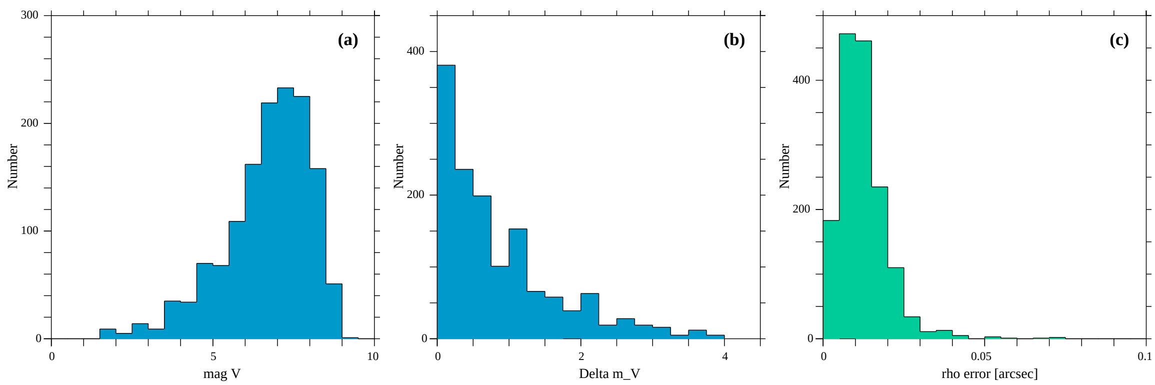

FIGURE 10. Distribution of m_V, Δm_V, and the errors σ_ρ of the measurements with PISCO in Merate.

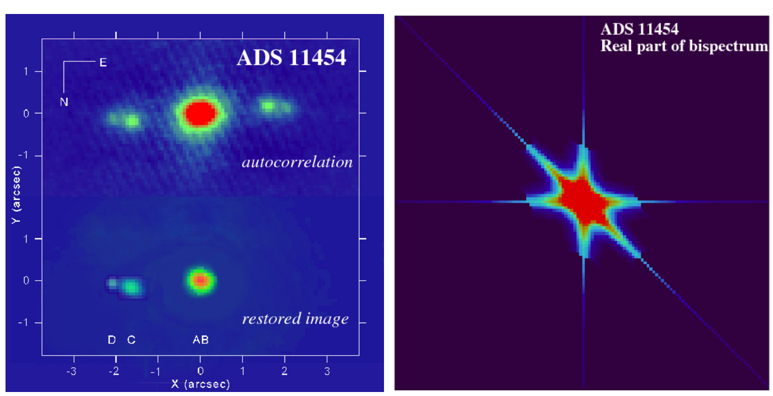

FIGURE 11. Example of the image restoration of ADS 11454 (left) from its bispectrum (right).

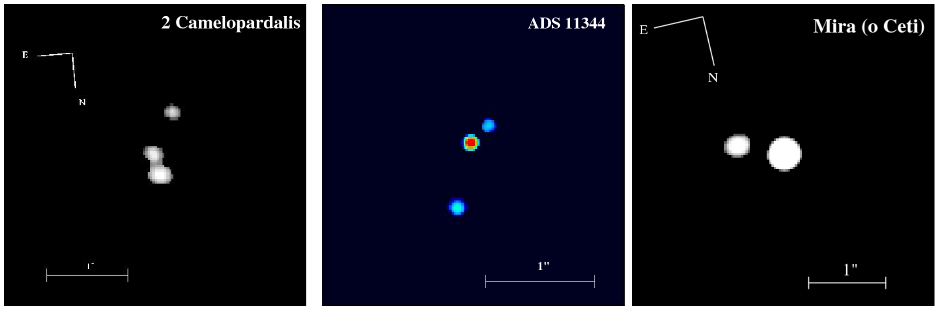

FIGURE 12. Examples of restored images from PISCO observations with bispectral methods.

TABLE 1. List of orbits computed from PISCO observations made in Merate.

Catalogue	ADS	Pub.	Catalogue	ADS	Pub.
A647	277	Inf. Circ. 164	STF1527	8128	MN, 395, 907
BU232	684	AN, 329, 54	STF1670AB	8630	AN, 328, 146
A1	1345	Inf. Circ. 159	STF1865AB	9343	Inf. Circ. 163
A2629	3610	AN, 329, 54	A1377	11468	Paper IX
STT98	3711	Inf. Circ. 165	STT359	11479	Inf. Circ.165
STF749	4209	MN, 374, 965	STF2437	11956	AN, 329, 54
BU560	4371	AN, 329, 54	STT363	11584	Inf. Circ. 165
STF3115	4376	AN, 329, 54	MCA55Aac	12540	AN, 329, 54
STT156	5447	MN, 357, 1255	A730	13850a	Paper IX
STF963AB	5514	Inf. Circ. 165	A730	13850b	Paper IX
STT213	7685	Inf. Circ. 166	H 1 48	14783	AN, 329, 54
STF1426AB	7730	AN, 329, 54	HU371	15115	MN, 367, 1170
STT216	7744	Inf. Circ. 168	STF2909AB	15971	Inf. Circ. 168
STT224	7871	MN, 395, 907	STF2909Aa-P	15971	Inf. Circ. 169
BU1076	7982	Inf. Circ. 166	STF2924AB	16057	Paper IX
BU1077 AB	8035	MN, 357, 1255	STT489AB	16538	Inf. Circ. 165

New orbits

Table 1 present the 32 new orbits computed using the PISCO measurements made in Merate in 2004-2008. Other 42 orbits were also computed with PISCO observations made at Pic du Midi in 1993–1998. We will illustrate this work with the example of γ Virginis that we particularly well monitored, especially around its periastron passage.

Indeed, the bright binary star γ Virginis illustrates the benefit of having a dedicated telescope capable of accurate measurement. The pair which has a period of 169 years passed through periastron in the spring of 2005 when the angular motion was 1 degree in 5 days (see Fig. 13).

Regular and precise measures by PISCO over several years (see Fig. 14) showed that the motion was Keplerian thus disproving the suggestion that there might be a third body in the system. The resulting orbital period was refined to an accuracy of 4 days and using the revised Hipparcos parallax the mass of the two F0 dwarf stars is 2.74 $M_\odot$ with

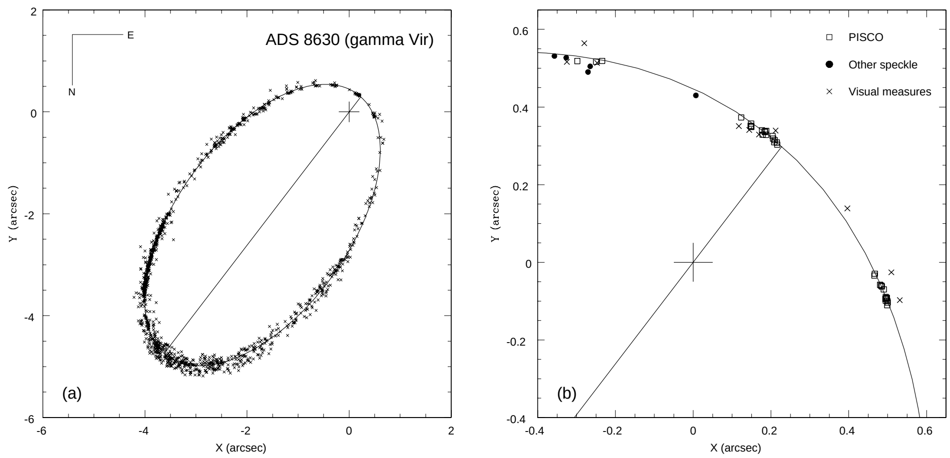

FIGURE 13. New orbit of ADS 8630: the measurements with PISCO are plotted as black dots.

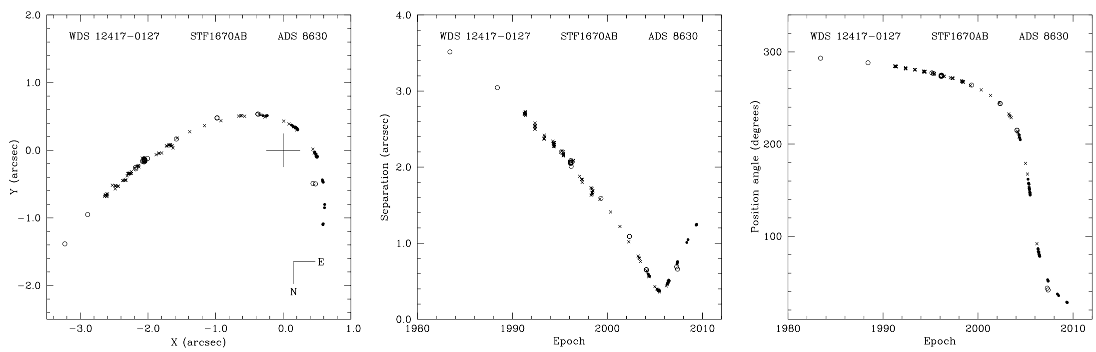

FIGURE 14. ADS 8630: the PISCO measurements (black dots) define a very precise track over the years, which is a proof of their good accuracy.

a formal error of 2.2%. Full details can be found in [11] and [13].

Zeta Aquari (ADS 15971) is also a very interesting case. This nearby ($d = 35pc$) visual binary exhibits periodic deviations from simple Keplerian motion (Fig. 15). Using all the photographic and speckle measurements published since 1923, we computed the residuals of our orbit of ADS 15971 AB in Cartesian coordinates, from which we derived the elements of the perturbation orbit Bb-P and its uncertainties with Hellerich (1925)'s least-squares method. To our knowledge, the uncertainties on those elements had never been computed before. The mass of the unseen companion is estimated at $M_b = 0.65\ M_\odot$ (see Paper VIII). The perturbation orbit Bb-P was very difficult to determine, because its major axis is very small: only 0".06 (see Table 2).

TABLE 2. New elements of the visual orbit AB and perturbation orbit Bb-P of ADS 15971 (Paper VIII.

Orbit	Ω_{2000} (°)	ω (°)	i (°)	e	T (yr)	P (yr)	n (°/yr)	a (")
AB	133.2	273.0	141.7	0.343	1982.733	486.70	0.7397	3.380
	±3.4	±9.4	±1.0	±0.029	±4.2	±40	±0.061	±0.023
Bb-P	20.9	330.3	22.3	0.125	2003.404	25.822	13.942	0.062
	±26	±29	±10	±0.018	±0.652	±0.139	±0.0751	±0.012

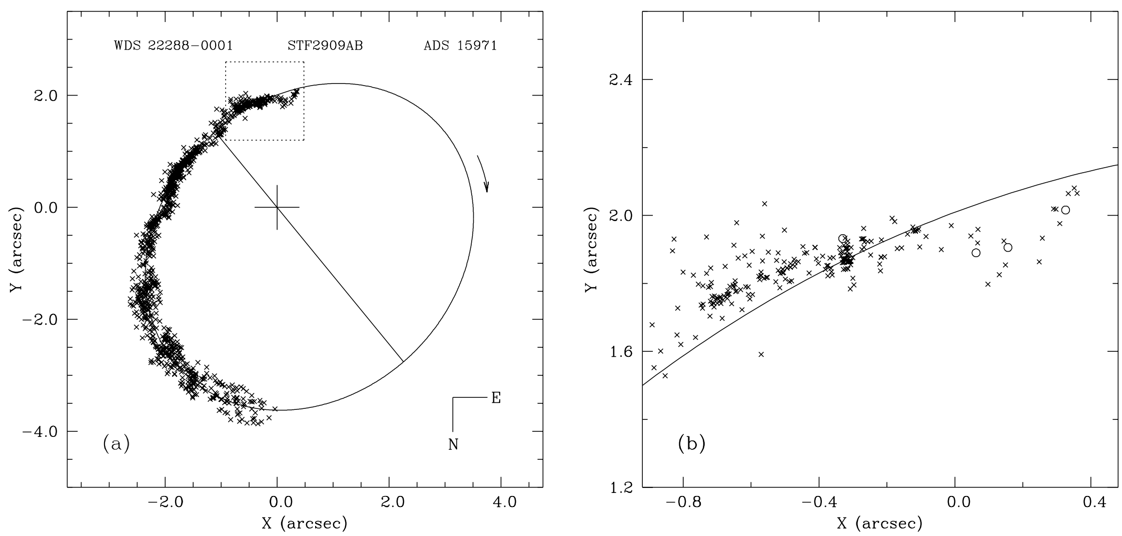

FIGURE 15. New orbit of ADS 15971 AB (a) with enlarged part in (b), corresponding to the dotted square in (a). Plotted as a solid line, it is actually the orbit of the center of mass of the Bb couple relative to the component A marked as a big cross. The observations of PISCO are printed as circles.

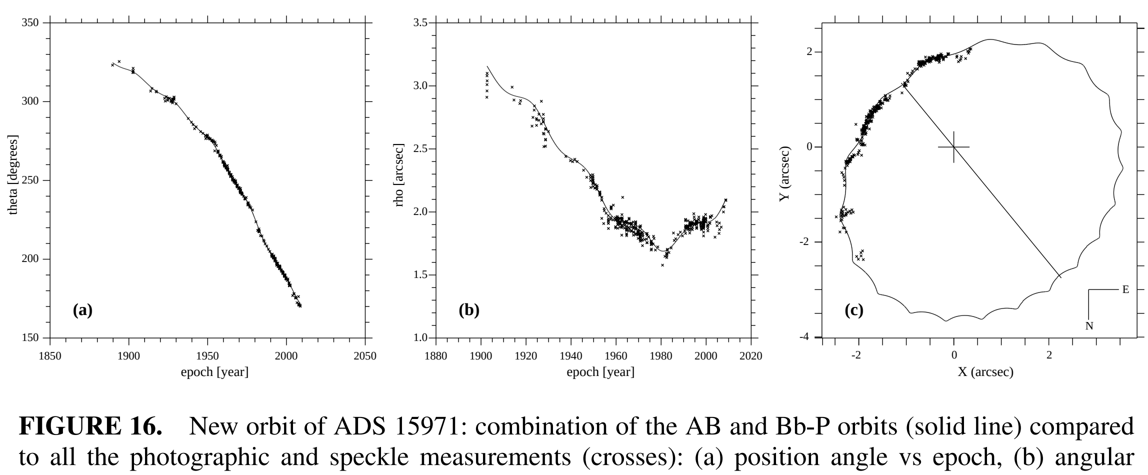

FIGURE 16. New orbit of ADS 15971: combination of the AB and Bb-P orbits (solid line) compared to all the photographic and speckle measurements (crosses): (a) position angle vs epoch, (b) angular separation vs epoch, and (c) orbit in the plane of the sky.

CONCLUSION AND PROSPECTS FOR THE FUTURE

Our program with PISCO has many assets. PISCO is a reliable, transportable, easy-to-use instrument, which has led to more than 2000 measurements with good astrometric accuracy (0".01, 0°.6). Absolute calibration was performed with a grating mask which makes our measurements independant of other observations. The Zeiss telescope is now the largest telescope in the world dedicated to the observation of visual binary stars. The availability of a dedicated telescope is essential for studying binary stars since it allows orbital monitoring during periastron passage. Our team is based on international collaborations and we are open to new collaborations. The observations with PISCO have led to 23 papers published in A&A, ApJ, PASP, MNRAS and AN from which 12 resulted from observations in Merate between 2004 and 2010

The project has already led to the determination of the orbits and mass sums of many visual binaries. More than 70 orbits were computed by our team using PISCO observations from which 32 orbits used measurements made in Merate. The accuracy of the masses found by will be largely improved when the distances are accurately known (Hipparcos was insufficient).

The long term aim is to improve visual orbits by improving the instrumentation available so that fainter pairs can be observed i.e. those towards the bottom of the Main Sequence. The PISCO team is now looking to improve both the efficiency of the detector and to increase the telescope aperture available. Negotiations are underway with the Observatoire de Cote d'Azur to use PISCO on the 1.5 metre MeO telescope at the Plateau de Calern in south-eastern France. Funding is being sought to purchase an EMCCD and the combination of these two factors will increase the magnitude limit available to PISCO by about 3 magnitudes allowing the measurement of closer and fainter binaries in particular those at the lower end of the main sequence.

REFERENCES

1. Aristidi, E., Carbillet, M., Lyon, J.-F., Aime, C., A&AS, 125, 139 (1997)
2. J. Hellerich, Astron. Nachr. 223, 335 (1925)
3. M. Kowalsky, Procès-verbaux de l'Université Imperiale de Kasan (1873)
4. A. Labeyrie, A&A, 6, 85 (1970)
5. C.D. Mackay, (http://www.ast.cam.ac.uk/ optics/Lucky_Web_Site/)
6. J.-L. Prieur, L. Koechlin, C. André, C. Gallou & C. Lucuix, *E*xperimental Astronomy, **8**, 297 (1998)
7. J.-L. Prieur, M. Scardia, L. Pansecchi, R.W. Argyle, M. Sala, M. Ghigo, L. Koechlin, E. Aristidi, *M*NRAS, **3**87, 772 (2008) (Paper V)
8. J.-L. Prieur, M. Scardia, L. Pansecchi, R.W. Argyle, M. Sala, (in preparation) (2010) (Paper IX)
9. M. Scardia, J.-L. Prieur, M. Sala, M. Ghigo, L. Koechlin, E. Aristidi, F. Mazzoleni, *M*NRAS, **357**, 1255, (2005) (Paper I)
10. M. Scardia, J.-L. Prieur, L. Pansecchi, R.W. Argyle, M. Sala, M. Ghigo, L. Koechlin, E. Aristidi, *M*NRAS, **3**67, 1170 (2006) (Paper II)
11. M. Scardia, R.W. Argyle, J.-L. Prieur, L. Pansecchi, S. Basso, N.M. Law and C.D. Mackay, *A*N, **3**28, 2, 146 (2007)
12. M. Scardia, J.-L. Prieur, L. Pansecchi, R.W. Argyle, S. Basso, M. Sala, M. Ghigo, L. Koechlin, E. Aristidi, *M*NRAS, **3**74, 965 (2007) (Paper III)

13. M. Scardia, J.-L. Prieur, L. Pansecchi, R.W. Argyle, S. Basso, N.M. Law and C.D. Mackay, Proceedings IAU Symposium 240, 132+558 (2007)
14. M. Scardia, J.-L. Prieur, L. Pansecchi, R.W. Argyle, M. Sala, S. Basso, M. Ghigo, L. Koechlin, E. Aristidi, *A*N, **3**29, 1, 54 (2008) (Paper IV)
15. M. Scardia, J.-L. Prieur, L. Pansecchi, R.W. Argyle, *A*N, **3**29, 4, 379 (2008)
16. M. Scardia, J.-L. Prieur, L. Pansecchi, R.W. Argyle, M. Sala, *A*N, **3**30, 1, 55 (2009) (Paper VI)
17. J.-L. Prieur, M. Scardia, L. Pansecchi, R.W. Argyle, M. Sala, *M*NRAS, **3**95, 907 (2009) (Paper VII)
18. M. Scardia, J.-L. Prieur, L. Pansecchi, R.W. Argyle, M. Sala, *A*N, (in press) (2010) (Paper VIII)
19. G. Weigelt, Opt. Comm., 21, 55 (1977)
20. S.P. Worden, K.S. Murray, G.D Schmidt, J.R.P. Angel, Icarus 32, 450 (1977)